Generalized lattice Wilson–Dirac fermions in (1+1) dimensions for atomic quantum simulation and topological phases

Kuno, Yoshihito; Ichinose, Ikuo; Takahashi, Yoshiro

CITATION:

Kuno, Yoshihito ...[et al]. Generalized lattice Wilson–Dirac fermions in (1+1) dimensions for atomic quantum simulation and topological phases. Scientific Reports 2018, 8: 10699.

ISSUE DATE:

2018-07-16

URL:

http://hdl.handle.net/2433/234224

SCIENTIFIC REPORTS

OPEN

Generalized lattice Wilson–Dirac fermions in (1 + 1) dimensions for atomic quantum simulation and topological phases

Received: 9 March 2018
Accepted: 5 July 2018
Published online: 16 July 2018

Yoshihito Kuno[1], Ikuo Ichinose[2] & Yoshiro Takahashi[1]

The Dirac fermion is an important fundamental particle appearing in high-energy physics and topological insulator physics. In particular, a Dirac fermion in a one-dimensional lattice system exhibits the essential properties of topological physics. However, the system has not been quantum simulated in experiments yet. Herein, we propose a one-dimensional generalized lattice Wilson-Dirac fermion model and study its topological phase structure. We show the experimental setups of an atomic quantum simulator for the model, in which two parallel optical lattices with the same tilt for trapping cold fermion atoms and a laser-assisted hopping scheme are used. Interestingly, we find that the model exhibits nontrivial topological phases characterized by gapless edge modes and a finite winding number in the broad regime of the parameter space. Some of the phase diagrams closely resemble those of the Haldane model. We also discuss topological charge pumping and a lattice Gross-Neveu model in the system of generalized Wilson-Dirac fermions.

The quantum simulation[1] of Dirac fermions is of fundamental importance because they are ubiquitous in theoretical physics. Dirac fermions appear in high-energy physics[2,3] and the condensed matter physics, e.g. topological matter[4], graphene physics, etc. In recent years, topological phases have become one of the most interesting subjects in physics, where Dirac fermions play an important key role[5,6]. In particular, a variety of one-dimensional (1D) lattice models have been extensively studied from the view point of nontrivial topological phases[7–13]. Experiments on cold atomic gases in an optical lattice have started to construct a "quantum simulator" of 1D topological models. Very recently, the experimental realization of a lattice topological model has been reported in ref.[14]. As one of the recent remarkable successes in experiments concerning 1D topological models, we note the realization of topological Thouless pumping[15,16] and a ladder topological model in a synthetic dimensional optical lattice[17].

Despite such experimental successes, the Dirac fermion model on a lattice called the Wilson-Dirac model[18] is still a toy model in the sense that it has not been realized and not yet quantum simulated in experiments. The 1D Wilson-Dirac model is the simplest and fundamental model that exhibits the essence of a topological insulator[5]. Thus, it is important to propose a quantum simulation for it and investigate its topological properties. Herein, we introduce a 1D generalized Wilson-Dirac model (GWDM) as an important quantum simulator. We propose feasible experimental setups for the 1D GWDM and investigate the phase diagram of the 1D GWDM theoretically, in particular, the locations of topological phases.

Schemes for realizing quantum simulators for the standard Dirac-fermion systems, using cold-atomic gases in continuum and lattice systems, have been already proposed. Some of them are a Raman coupling scheme[19–22], a modulation method on a tilted lattice[23], and an effective model of two-component cold atoms in a 1D optical superlattice[24]. The above works focus on the standard Dirac fermions. In this work, we are interested in constructing a quantum simulator for extended lattice Wilson-Dirac fermions, which include the ordinary Wilson-Dirac fermions on the lattice as a specific case and has a large parameter space to be realized by experiments. The 1D GWDM, which contains nontrivial phases in the hopping terms, is an interesting model by itself because these phases work as free parameters that change the physical properties of the ordinary Wilson-Dirac fermion

[1]Department of Physics, Graduate School of Science, Kyoto University, Kyoto, 606-8502, Japan. [2]Department of Applied Physics, Nagoya Institute of Technology, Nagoya, 466-8555, Japan. Correspondence and requests for materials should be addressed to Y.K. (email: ykuno@yagura.scphys.kyoto-u.ac.jp)

model, e.g. the symmetries of the Hamiltonian, the energy spectrum, the ground state including nontrivial topological phases, etc. Actually, in the experimental setups for the 1D GWDM, the phases can be controlled by a laser-assisted hopping scheme, which is familiar in experiments on cold atomic systems.

In order to realize the Dirac fermions by cold atomic gases in an optical lattice, the greatest difficulty is the creation of the Dirac-gamma matrices from the nearest-neighbor (NN) hopping amplitudes of cold atoms. To this end, we use two different internal states of a fermionic atom and two parallel "tilted" optical lattices. This setup is an important platform for realizing the 1D GWDM. In particular, we explain a general scheme for the generation of Dirac-gamma matrices by using a laser-assisted hopping technique. Furthermore, to understand the general construction scheme, we propose a concrete set up by using ^{171}Yb atoms. After that, we study the symmetry properties and the topological phases of the 1D GWDM and provide the expected ground-state phase diagrams. Finally, we put $\hbar = 1$ throughout this paper.

Results

Generalized Wilson-Dirac fermions. As explained in the introduction, we consider two internal states for a single fermion and denote them by $\Psi_j = (a_j, b_j)^t$ at lattice site j. The GWDM in a 1D spatial lattice is defined by the following Hamiltonian,

$$\begin{aligned} H^{(g)}_{\mathrm{GWDM}} &= \sum_j \Psi_j^\dagger \Gamma_z(\Delta)\Psi_j - \sum_j [\Psi_{j+1}^\dagger \Gamma_z^h(\theta_a, \theta_b)\Psi_j + \mathrm{h.c.}] \\ &\quad + \sum_j [\Psi_{j+1}^\dagger \Gamma_x(\theta^+, \theta^-)\Psi_j + \Psi_{j+1}\Gamma_x^*(\theta^+, \theta^-)\Psi_j^\dagger], \end{aligned} \tag{1}$$

with

$$\Gamma_z(\Delta) = \begin{bmatrix} \Delta & 0 \\ 0 & -\Delta \end{bmatrix} = \Delta\sigma_z, \tag{2}$$

$$\Gamma_z^h(\theta_a, \theta_b) = \begin{bmatrix} |J_a|e^{i\theta_a} & 0 \\ 0 & |J_b|e^{i\theta_b} \end{bmatrix}, \tag{3}$$

$$\Gamma_x(\theta^+, \theta^-) = \begin{bmatrix} 0 & |J_{ab}^-|e^{i\theta^-} \\ |J_{ab}^+|e^{-i\theta^+} & 0 \end{bmatrix}, \tag{4}$$

$$\Gamma_x^*(\theta^+, \theta^-) = \begin{bmatrix} 0 & |J_{ab}^-|e^{-i\theta^-} \\ |J_{ab}^+|e^{i\theta^+} & 0 \end{bmatrix}, \tag{5}$$

where σ_z is the Pauli matrix, θ_a, θ_b, θ^+, and θ^- are site-independent phases, Δ is an energy-offset; and $|J_a|$, $|J_b|$, $|J_{ab}|$ and $|J_{ab}^-|$ are hopping amplitudes. The different internal states a_j and b_j originate from, e.g. an internal spin, and have different energy levels. In this case, the energy splitting is nothing but a hyperfine energy splitting, which can be created by the Zeeman effect in an external magnetic field.

We express the model in Eq. (1) in terms of the fermion creation and annihilation operators $a_j^\dagger(a_j)$ and $b_j^\dagger(b_j)$, as

$$H^{(g)}_{\mathrm{GWDM}} = H_{\mathrm{spinOL}} + H_{\mathrm{ahop}} + H_{\mathrm{bhop}} + H_{ab}^+ + H_{ab}^-, \tag{6}$$

$$H_{\mathrm{spinOL}} = \sum_{j=1} \Delta(a_j^\dagger a_j - b_j^\dagger b_j), \tag{7}$$

$$H_{\mathrm{ahop}} = -\sum_j J_a a_{j+1}^\dagger a_j + \mathrm{h.c.}, \tag{8}$$

$$H_{\mathrm{bhop}} = -\sum_j J_b b_{j+1}^\dagger b_j + \mathrm{h.c.}, \tag{9}$$

$$H_{ab}^+ = \sum_j J_{ab}^+ a_j^\dagger b_{j+1} + \mathrm{h.c.} \tag{10}$$

$$H_{ab}^- = \sum_j J_{ab}^- a_j^\dagger b_{j-1} + \mathrm{h.c.}, \tag{11}$$

where $J_a = |J_a|e^{i\theta_a}$, $J_b = |J_b|e^{i\theta_b}$, $J_{ab}^+ = |J_{ab}|e^{i\theta^+}$, and $J_{ab}^- = |J_{ab}^-|e^{i\theta^-}$. In the following section, we shall show feasible methods for constructing each term in the above Hamiltonian $H^{(g)}_{\mathrm{GWDM}}$ in experiments on ultra-cold fermion

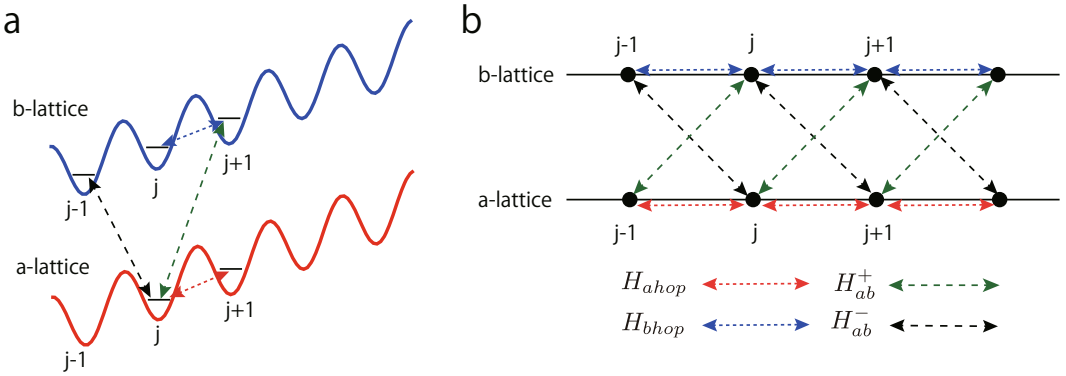

Figure 1. (**a**) Two parallel optical lattice. Each lattice traps a different internal state of fermion. The two lattices have the same tilt. (**b**) Four types of hopping term. In the exchange hopping term denoted by the black and green dashed arrows, the fermionic atoms hop to a different site in a different optical lattice with changing the internal spin.

gases. Before detailing the theoretical proposal, we note that by setting the hopping amplitudes as $|J_a| = |J_b| = t$ and $|J_{ab}^{+}| = |J_{ab}^{-}| = t'$ and the phases as $\theta_a = 0$, $\theta_b = \pi$ and $\theta^{+} = -\theta^{-} = -\pi/2$, the Hamiltonian in Eq. (1) reduces to the (1 + 1) D version of the ordinary Wilson-Dirac fermion model[18], in which the Dirac gamma matrices are given by $\gamma_0 = \sigma_z$, $\gamma_1 = \sigma_y$ and $\gamma_5 = \gamma_0\gamma_1$, respectively. It should be emphasized that the phase conditions, $\theta_a = 0$, $\theta_b = \pi$ and $\theta^{+} = -\theta^{-} = -\pi/2$ can be realized in real experiments by tuning the incident angle of Raman lasers. Hereafter, we call these conditions the *Dirac condition*.

Theoretical proposal for quantum simulation. Let us explain the general setup scheme for the Hamiltonian in Eq. (1) by ultra-cold atomic gases. To this end, we use two different internal states of a single fermionic atom in an optical lattice. In particular, the most important problem is the creation of the generalized gamma matrices in the Hamiltonian $H_{GWDM}^{(g)}$ given by Eqs (2)–(5). Generally speaking, the experimental setup consists of three steps: (i) prepare two different internal states of a fermionic atom and set two parallel deep optical lattices with the same tilt. (ii) apply four types of laser-assisted hopping that generate the matrices in Eqs (2)–(5) by using some excitation lasers in addition to the off-resonant laser of the optical lattice, and (iii) tune the intensity and frequency of the excitation lasers and set the appropriate incident angle of the excitation lasers to realize the uniform phase condition.

In order to clarify the above setup, we shall explain each step in detail in the rest of this section.

Two parallel optical lattice. In our proposal, we first prepare the two internal states of the fermionic atom denoted by $|a\rangle$ and $|b\rangle$ and consider two 1D parallel optical lattices with the same tilt[25,26]. Each optical lattice can trap one of two states, $|a\rangle$ or $|b\rangle$. Then, we set the optical lattices sufficiently deep to suppress the natural hopping process between NN lattice sites. Here, we call the optical lattice trapping the state $|a\rangle$ the "a-lattice" and the other optical lattice trapping the state $|b\rangle$ the "b-lattice". We apply the tight-binding picture to each optical lattice system and assume that the potential minimums of the two lattices exist at the same locations[27]. The lattice site label j is used for the a- and b-lattices as shown in Fig. 1(a), i.e. the a- and b-lattices comprise a parallel optical lattice system. In this system, by choosing two appropriate internal levels of the fermionic atom $|a\rangle$ and $|b\rangle$, an energy-offset Δ_{ab} at site j can be generated. In the second-quantized tight-binding picture, the energy-offset Δ_{ab} leads to $\sum_i \frac{\Delta_{ab}}{2}(a_j^{\dagger}a_j - b_j^{\dagger}b_j)$, where the tight-binding operators of $|a\rangle$ and $|b\rangle$ are regarded as the operators a_j and b_j defined in the previous section. Therefore, the energy-offset part H_{spinOL} of Eq. (7) is identified as $\Delta = \Delta_{ab}/2$.

Four types of laser-assisted hopping. For the realization of the hopping terms in Eqs (8)–(11), we apply four types of laser-assisted hopping to the two parallel optical lattice system. Laser-assisted hopping is created by the Λ-shaped scheme explained in Methods. By using the two parallel lattices, which are tilted by the same amount by certain experimental techniques, the tilted energy difference Δ_t between the NN lattice can be introduced. We denote the four types of hopping corresponding to Eqs (8)–(11) by $\Lambda_{a_{j+1}}^{a_j}$, $\Lambda_{b_{j+1}}^{b_j}$, $\Lambda_{b_{j+1}}^{a_j}$ and $\Lambda_{b_{j-1}}^{a_j}$. For example, the label on $\Lambda_{a_{j+1}}^{a_j}$ means the NN hopping between a_j and a_{j+1} on the a-lattice, which corresponds to the hopping term in Eq. (8) as shown in Fig. 1(a,b). The other labels have the similar meanings.

Next, to establish $\Lambda_{a_{j+1}}^{a_j}$, $\Lambda_{b_{j+1}}^{b_j}$, $\Lambda_{b_{j+1}}^{a_j}$ and $\Lambda_{b_{j-1}}^{a_j}$ without interfering with each other, suitable tunings of the on-site energy-offset, the lattice tilt and the excitation laser frequencies used in the laser-assisted hopping amplitudes are required. One can directly create $\Lambda_{a_{j+1}}^{a_j}$ and $\Lambda_{b_{j+1}}^{b_j}$ by choosing an appropriate excited state for each state. However, $\Lambda_{b_{j+1}}^{a_j}$ and $\Lambda_{b_{j-1}}^{a_j}$ have to be carefully prepared because we need to prohibit or highly suppress the Rabi coupling $a_j^{\dagger}b_j + a_jb_j^{\dagger}$ at the same site. Furthermore, in the case where the two component fermionic atom originates from different z-components of the internal spin, we must select the appropriate polarization of the excitation lasers in creating $\Lambda_{b_{j+1}}^{a_j}$ and $\Lambda_{b_{j-1}}^{a_j}$. To satisfy these requirements, we show the general tuning condition as the energy dia-

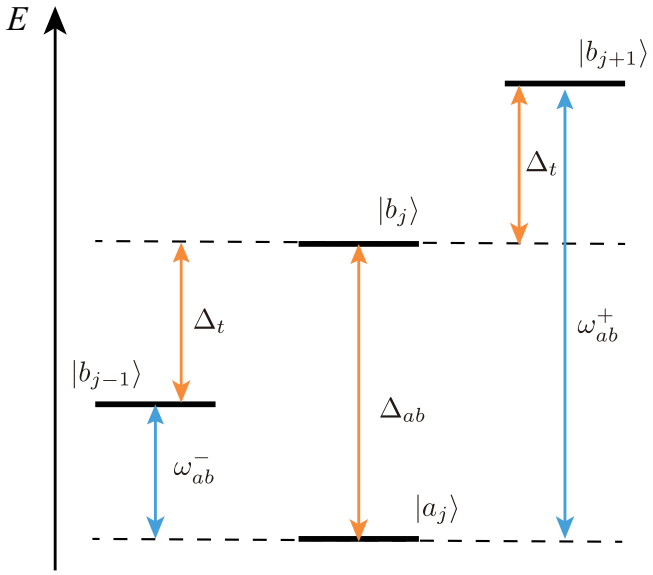

Figure 2. Energy condition for realizing the laser-assisted hopping $\Lambda_{b_{j+1}}^{a_j}$ and $\Lambda_{b_{j-1}}^{a_j}$.

gram shown in Fig. 2, where, $|a_j\rangle$, $|b_j\rangle$, $|b_{j+1}\rangle$, and $|b_{j-1}\rangle$ are two different internal states of an atom on lattice sites j, $j+1$ and $j-1$, respectively. The energy splitting Δ_{ab} between $|a_j\rangle$ and $|b_j\rangle$ is related to the on-site energy-offset $2\Delta = \Delta_{ab}$, as explained before. $\omega_{ab}^{+} = \Delta_{ab} + \Delta_t$ is the frequency difference of the two excitation lasers used in the laser-assisted hopping $\Lambda_{b_{j+1}}^{a_j}$. (For a detailed definition, see Methods.) $\omega_{ab}^{-} = \Delta_{ab} - \Delta_t$ is the corresponding quantity of $\Lambda_{b_{j-1}}^{a_j}$. To realize $\Lambda_{b_{j+1}}^{a_j}$ and $\Lambda_{b_{j-1}}^{a_j}$ independently, we need to impose the following condition: $\Delta_{ab} > \Delta_t \gg \delta_b^{+(-)}$, where $\delta_b^{+(-)}$ is the two photon detuning used in the laser-assisted hopping $\Lambda_{b_{j+1}}^{a_j}$ ($\Lambda_{b_{j-1}}^{a_j}$). Actually, we take $\delta_b^{+(-)}$ to be zero to create a resonance between NN sites. Then, in order to sufficiently separate the resonance conditions of $\Lambda_{b_{j+1}}^{a_j}$ and $\Lambda_{b_{j-1}}^{a_j}$, the difference between the two resonance denoted by $\omega_{ab}^{+} - \omega_{ab}^{-} = 2\Delta_t$ should be large compared with the two-photon Rabi frequency in Eq. (29). If these conditions are satisfied in the two parallel optical lattices, the transition probability of the same site is negligibly small (at least strongly suppressed). Then, $\Lambda_{b_{j+1}}^{a_j}$ and $\Lambda_{b_{j-1}}^{a_j}$ are dominant.

As explained above, by applying the four types of laser-assisted hopping $\Lambda_{a_{j+1}}^{a_j}$, $\Lambda_{b_{j+1}}^{b_j}$, $\Lambda_{b_{j+1}}^{a_j}$ and $\Lambda_{b_{j-1}}^{a_j}$ to the two parallel optical lattices with the same tilt, we can design the hopping terms in Eqs (8)–(11). Therefore, we can produce a quantum simulator of the 1D GWDM.

Furthermore, controlling the parameters of the excitation lasers enables us to set the uniform phases θ_a, θ_b, θ^+, and θ^- and the uniform hopping amplitudes rather freely.

Concrete example using ^{171}Yb. In general, the above theoretical proposal can be performed by using some atomic species, e.g. alkali atoms. As one candidate, we consider ^{171}Yb atoms. In particular, we employ the two internal states of ^{171}Yb, $|^1S_0, F_z = 1/2\rangle$ and $|^1S_0, F_z = -1/2\rangle$ as two component fermionic state, i.e.

$$|^1S_0, F_z = 1/2\rangle \to |a\rangle, \quad |^1S_0, F_z = -1/2\rangle \to |b\rangle.$$

Then, the energy splitting Δ_{ab} can be generated and controlled by a uniform magnetic fields, i.e. $\Delta_{ab} \to \Delta_{ab}(B_0)$. Actually, the nuclear g-factor of ^{171}Yb is 0.985; therefore, the value of Δ_{ab} is set to be 75 kHz with a magnetic field of 100 G. Furthermore, to create $\Lambda_{a_{j+1}}^{a_j}$, $\Lambda_{b_{j+1}}^{b_j}$, $\Lambda_{b_{j+1}}^{a_j}$ and $\Lambda_{b_{j-1}}^{a_j}$, we have to select the appropriate four sets of three states $\{|A\rangle, |B\rangle, |E\rangle\}$ in the Λ-shaped scheme. (See Methods.) Here, we show the selection of the ^{171}Yb internal states in Table 1. Here, the (L_A, L_B) line in Table 1 expresses the pattern of polarization of the two excitation lasers. (The excitation lasers with π or $\sigma^{\pm}$ polarization are considered here.) $\Lambda_{b_{j+1}}^{a_j}$ and $\Lambda_{b_{j-1}}^{a_j}$ can be controlled independently. Furthermore, $\Lambda_{a_{j+1}}^{a_j}$ and $\Lambda_{b_{j+1}}^{b_j}$ can be independently controlled since the two excited states $|^3P_1, F_z = 1/2\rangle$ and $|^3P_1, F_z = -1/2\rangle$ can be well separated on the order of 100 MHz with magnetic field having a reasonable strength about 100 G. Figure 3 shows schematics of the four types of laser-assisted hopping corresponding to Table 1. The energy difference between the two excited states and the natural widths of the two excited states are denoted by ω_z, Γ_{E_1} and Γ_{E_2}, respectively. Then, the detuning δ for each type of laser-assisted hopping is allowed to satisfy $\Gamma_{E_1}, \Gamma_{E_2} \ll \delta \ll \omega_z$ since $\omega_z/(2\pi) = 100$ [MHz] and $\Gamma_{E_{1(2)}}/(2\pi) \sim 200$ [kHz]. This condition allows an independent laser assisted hopping scheme. The mutual interference could be suppressed to be on the order of $\delta/\omega_z \ll 0.1$. That is, the four types of laser-assisted hopping can be produced independently. Here, we comment that the overlap integral $\tilde{J}_{j,j+1}$, which is explicitly defined in Eq. (29) in Methods, depends on the shape and location of the potential minimum of the Wannier functions in the $^3P_1$ excited states, which are used in the four types

	Λ^{aj}_{aj+1}	Λ^{bj}_{bj+1}	Λ^{aj}_{bj+1}	Λ^{bj}_{bj-1}
$\|A\rangle$	$^1S_0, F_z=1/2$	$^1S_0, F_z=-1/2$	$^1S_0, F_z=1/2$	$^1S_0, F_z=1/2$
$\|B\rangle$	$^1S_0, F_z=1/2$	$^1S_0, F_z=-1/2$	$^1S_0, F_z=-1/2$	$^1S_0, F_z=-1/2$
$\|E\rangle$	$^3P_1, F_z=1/2$	$^3P_1, F_z=-1/2$	$^3P_1, F_z=-1/2(1/2)$	$^3P_1, F_z=-1/2(1/2)$
(L_A, L_B)	(π, π)	(π, π)	$(\sigma(\pi), \pi(\sigma))$	$(\sigma(\pi), \pi(\sigma))$

Table 1. Four types of laser-assisted hopping by using the hyperfine structure of ^{171}Yb.

of laser-assisted hopping. Generally, to make $\tilde{J}_{j,j+1}$ have a finite and reasonably large value, the location of the potential minimum needs to be set on the potential maximum of the $^1S_0$ lattice[28,29]. Furthermore, the Wannier function of the excited states needs to be sufficiently broad so that the overlap integral has a sufficiently large value. To this end, the relation between the polarization of the $^3P_1$ excited states, denoted by α_P, and that of $^1S_0$, denoted by α_S, plays an important key role. If $|\alpha_P| - |\alpha_S| < 0$ and $\mathrm{sgn}(\alpha_P) = -\mathrm{sgn}(\alpha_S)$, the above requirement is satisfied. In fact, the Yb atom satisfies the conditions for typical wave-lengths of optical lattice lasers, e.g. 532 nm and 1064 nm, etc[30,31]. Therefore, the overlap integral between the $^1S_0$ and $^3P_1$ Wannier functions can be sufficiently large.

Phase diagram and topological phase. As a next step, we study whether or not the GWDM has nontrivial topological phases. The system contains the uniform phases θ_a, θ_b, θ^+, and θ^-, then, we shall clarify their parameter regime corresponding to topological phases. In what follows, we regard θ_a, θ_b, θ^+, and θ^- as free parameters. The above phases are fully tunable in real experiments; see Methods.

To discuss the above problem, we first study the symmetries of the GWDM by using the symmetry-classification scheme in refs[32,33]. The symmetries of the system depend on the phases $\{\theta\}$. We shall also obtain the energy spectrum of the GWDM on a finite lattice with open boundary condition (OBC). Then, the spectrum is expected to exhibit zero-energy edge states in some parameter regime of the phases $\{\theta\}$. The existence of the zero-energy edge states is a direct signal of a nontrivial topological phase in the bulk system by the bulk-edge correspondence.

Hereafter for simplicity, we impose conditions for the hopping amplitudes in Eqs (8)–(11) such as $|J_a| = |J_b| = |J^+_{ab}| = |J^-_{ab}| = 1$ as they do not change the physical results. The above condition again can be realized in certain experimental setups[34].

We consider the system under periodic boundary condition, which preserves the discrete translational symmetry. We first focus on the symmetries of the bulk Hamiltonian and also the bulk topological properties of the GWDM. The bulk-momentum Hamiltonian $H_{\mathrm{bulk}}(k)$ is obtained from Eq. (1) as,

$$H_{\mathrm{bulk}}(k) = \begin{bmatrix} \Delta - 2\cos(k+\theta_a) & e^{-ik+i\theta^+} + e^{ik+i\theta^-} \\ e^{-ik-i\theta^-} + e^{ik-i\theta^+} & -\Delta - 2\cos(k+\theta_b) \end{bmatrix}, \tag{12}$$

where we have taken the lattice spacing as the length unit. Under the Dirac conditions $\theta_a = 0$, $\theta_b = \pi$, and $\theta^+ = -\theta^- = \pi/2$, $H_{\mathrm{bulk}}(k)$ is just the bulk-momentum Hamiltonian of the ordinary Wilson-Dirac fermion:

$$H_{\mathrm{bulk}}(k) = [\Delta - 2\cos k]\sigma_z + [2\sin k]\sigma_x \equiv \mathrm{d}(k)\cdot\sigma, \tag{13}$$

where $\mathrm{d}(k) = (d_x, d_z) = (2\sin k, \Delta - 2\cos k)$. This is the base model of 1D topological insulator[5] and belongs to the BDI class Hamiltonian. [See later discussion.] Then, the nontrivial topological phase can be characterized by the winding number N_w[6], which is obtained by integrating the vector trajectory of $\mathrm{d}(k)$ defined by,

$$N_w = \int_{-\pi}^{\pi} \frac{dk}{2\pi} \frac{\boldsymbol{d}(k)}{|\boldsymbol{d}(k)|} \times \frac{d}{dk}\left(\frac{\boldsymbol{d}(k)}{|\boldsymbol{d}(k)|}\right). \tag{14}$$

For a nontrivial topological phase, $N_w = +1$ or -1, whereas for a trivial insulating phase $N_w = 0$. In the parameter regime $-2 \le \Delta \le 2$, a nontrivial topological phase with $N_w = +1$ is known to exist[5,6].

We shall also consider the finite lattice system of the 1D GWDM with OBC later and show the existence of degenerate zero-energy edge states by diagonalizing the Hamiltonian of the 1D lattice system with the system size $L = 100$ (generally, we take L to be an even integer). The zero-energy edge state is a direct signal of the existence of nontrivial topological phases.

Symmetries, topological phases and zero-energy edge modes in the 1D GWDM. We shall show how to construct topologically nontrivial Hamiltonians in the 1D GWDM, and provide the experimental conditions for the laser setups to realize them. As classification theory indicates[32,33], a 1D model, which has nontrivial topological phases, belongs to the BDI or AIII class. This means that the 1D model must at least possess chiral symmetry[35]. The relevant symmetries are the time-reversal symmetry ($\mathcal{T}$) and charge-conjugation symmetry ($\mathcal{C}$) for the classification scheme. The system has time-reversal symmetry if and only if the Hamiltonian H satisfies the following condition;

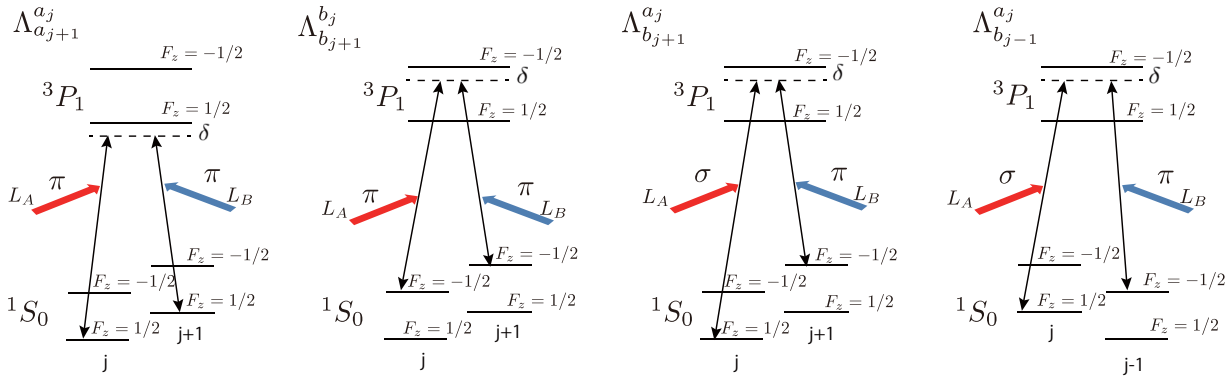

Figure 3. Schematics of four types of laser-assisted hopping in the ^{171}Yb atom system. The energy difference between the NN sites (j and $j\pm1$), and that between $F_z=1/2$ and $F_z=-1/2$ in the $^1S_0$ manifold at the same site are $\pm\Delta_i$ and Δ_{ab}, respectively. The detunings for the excited states take the same value δ.

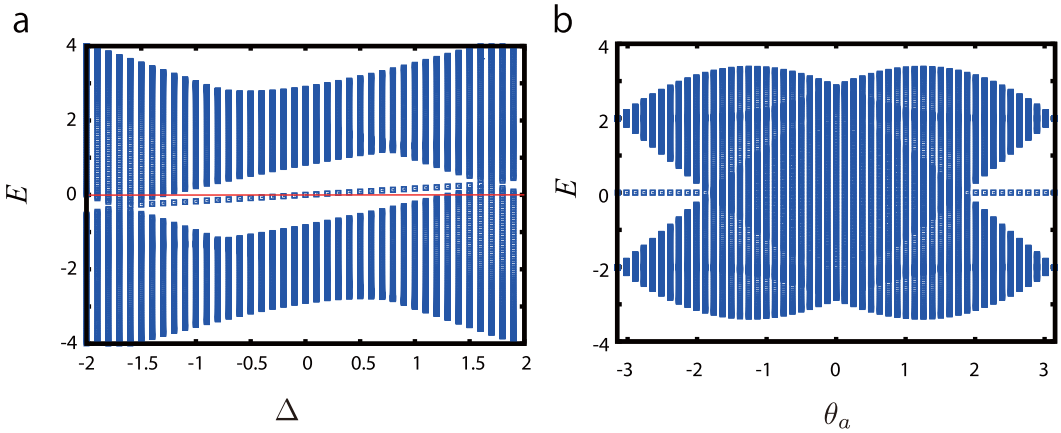

Figure 4. (**a**) Energy spectra for $\theta_a=3\pi/4$ and $\theta_b=0$. (**b**) Energy spectra for $\Delta=0$ and $\theta_b=0$.

$$\mathcal{T}: U_T^\dagger \mathcal{K} H \mathcal{K} U_T = U_T^\dagger H^* U_T = H, \tag{15}$$

where U_T is a unitary operator and $\mathcal{K}$ is the complex-conjugation operator. Similarly, for charge-conjugation symmetry (particle-hole symmetry),

$$\mathcal{C}: U_C^\dagger \mathcal{K} H \mathcal{K} U_C = U_C^\dagger H^* U_C = -H, \tag{16}$$

where U_C is again a unitary operator. The BDI class has $\mathcal{T}$ and $\mathcal{C}$ symmetries with $\mathcal{T}^2=+1$ and $\mathcal{C}^2=+1$, whereas the AIII class has only $\mathcal{S}\equiv\mathcal{T}\cdot\mathcal{C}$ symmetry, which is called chiral symmetry. Under $\mathcal{K}$, k and θ's transform as (k, θ's) $\rightarrow -$(k, θ's). Then, it is seen that the Hamiltonian of the ordinary Wilson-Dirac fermion [Eq. (13)] has both time-reversal and charge-conjugation symmetries with $U_T=\sigma_z$ and $U_C=\sigma_x$, respectively. From the time-reversal and charge conjugation operators, the chiral operator is directly obtained as $U_S=\sigma_y$.

To search the parameter regime of the chiral symmetric Hamiltonian in the 1D GWDM, we first assume the Dirac condition, i.e. $\theta^+=-\pi/2$ and $\theta^-=\pi/2$, but relax θ_a and θ_b as free parameters. Then, we show the typical behavior of the energy spectra of the finite lattice system including the edge modes. In Fig. 4(a), we plot the energy spectra for $\theta_a=3\pi/4$ and $\theta_b=0$ by varying the parameter Δ. The results show the spectrum of the edge modes is located at the center of the spectra. A close look at the calculations reveals that the edge modes have non-vanishing energies, except for $\Delta=0$ and the spectrum tilts along Δ. This indicates that the present system does not have chiral symmetry, except in the case of $\Delta=0$.

To study further, by fixing $\theta_b=0$ and $\Delta=0$, we calculate energy spectra by varying the parameter θ_a. The results are shown in Fig. 4(b). We find interesting behavior in the regimes of $-\pi\le\theta_a\le-\pi/2$ and $\pi/2\le\theta_a\le\pi$, i.e. the zero-energy edge modes survive as long as the bulk-gap does not close.

It is instructive to visualize the energy spectrum of the bulk system obtained from the bulk Hamiltonian $H_{\text{bulk}}(k)$ in Eq. (12). For arbitrary θ_a and θ_b with $\Delta=0$, the bulk energy spectrum $E_\pm(k)$ is obtained as,

$$E_{\pm}(k) = -(\cos(k+\theta_a) + \cos(k+\theta_b)) \pm [(\cos(k+\theta_a) + \cos(k+\theta_b))^2 - 4\cos(k+\theta_a)\cos(k+\theta_b) - 4\sin^2 k]^{\frac{1}{2}}. \quad (17)$$

when the first term on the right-hand side (RHS) of Eq. (17) is non-vanishing, the spectrum is asymmetric, i.e. $E_{+}(k) \neq -E_{-}(k)$, this means that the spectrum is non-relativistic. On the other hand, once the first term vanishes, the spectrum is symmetric around $E=0$, i.e. $E_{+}(k) = -E_{-}(k)$. The spectrum is the relativistic (massive) Dirac type. From this consideration, in order to make the 1D GWDM chiral symmetric, we should impose a condition such as

$$\theta_a = \theta_b \pm \pi. \quad (18)$$

hereafter, we call Eq. (18) the chiral symmetry (CS) condition. This observation of the bulk energy spectra gives an important insight about the parameter regime of the topologically nontrivial Hamiltonian in the GWDM as well as the above numerical results of the edge modes in the finite system.

Let us focus our attention on the CS case of the bulk Hamiltonian by setting $\theta_a = \theta_b \pm \pi$ in Eq. (12);

$$H^{\mathrm{CS}}_{\mathrm{bulk}}(k) = [\Delta - 2\cos(k+\theta_a)]\sigma_z + [\cos(-k+\theta^+) + \cos(k+\theta^-)]\sigma_x + [\sin(-k+\theta^+) + \sin(k+\theta^-)]\sigma_y. \quad (19)$$

As the Hamiltonian $H^{\mathrm{CS}}_{\mathrm{bulk}}(k)$ in Eq. (19) contains all three components of the Pauli matrices, one may think that it cannot be chiral symmetric unless further conditions are imposed. However, we shall show that it is not only chiral symmetric but also time-reversal and charge-conjugate symmetric. To this end, we introduce the rotated Pauli matrix $\tilde{\sigma}_j(\rho)$ defined as follows (see Methods):

$$\tilde{\sigma}_j(\rho) \equiv \exp\left(-i\frac{\rho}{2}\sigma_i\right)\sigma_j \exp\left(i\frac{\rho}{2}\sigma_i\right) = \sigma_j \cos\rho + \varepsilon_{ijk}\sigma_k \sin\rho, \quad (20)$$

where ε_{ijk} is the totally anti-symmetric tensor, i.e. $\varepsilon_{xyz}=1$, etc. By using the rotated Pauli matrix $\tilde{\sigma}_x(\rho)$, it can be shown that $H^{\mathrm{CS}}_{\mathrm{bulk}}(k)$ is expressed as,

$$H^{\mathrm{CS}}_{\mathrm{bulk}}(k) = [\Delta - 2\cos(k+\theta_a)]\sigma_z + \left[2\cos\left(k - \frac{\theta^+ - \theta^-}{2}\right)\right]\tilde{\sigma}_x\left(\frac{\theta^+ + \theta^-}{2}\right). \quad (21)$$

This expression shows that the system Hamiltonian $H^{\mathrm{CS}}_{\mathrm{bulk}}(k)$ possesses time-reversal and charge-conjugation symmetries. In fact, for time-reversal symmetry,

$$U_T = \exp[i(\theta^+ + \theta^-)\sigma_z], \quad (22)$$

and for charge-conjugation symmetry,

$$U_C = \sigma_y \exp[i(\theta^+ + \theta^-)\sigma_z]. \quad (23)$$

We note that from the above consideration, the CS condition is an important condition for the BDI class bulk-momentum Hamiltonian. That is, the CS condition in Eq. (18) is a sufficient condition for the BDI class in our quantum simulator of the 1D GWDM. This means that *we do not need to implement the ordinary 1D Wilson-Dirac fermion in the atomic simulator to simulate the topological properties of the Dirac model.*

We turn to the investigation of the phase diagram including nontrivial topological phases under the CS condition. It is expected that interesting results are obtained because the additional phase parameters enlarge the regime of topological phases from that of the standard Wilson-Dirac model.

By shifting the wave vector as $k \to k + (\theta^+ - \theta^-)/2$, the Hamiltonian $H^{\mathrm{CS}}_{\mathrm{bulk}}(k)$ is expressed as

$$H^{\mathrm{CS}}_{\mathrm{bulk}}(k) = \left[\Delta - 2\cos\left(k + \theta_a + \frac{\theta^+ - \theta^-}{2}\right)\right]\sigma_z + [2\cos k]\tilde{\sigma}_x((\theta^+ + \theta^-)/2). \quad (24)$$

Then, the Bloch vector is given by the following general form with an angle α:

$$\mathrm{d}(k) = (d_x(k), d_z(k)) \equiv (2\cos k, \Delta - 2\cos(k-\alpha)),$$

where $\alpha = -\theta_a - (\theta^+ - \theta^-)/2$ in the present case. We calculate the energy spectrum of the 1D GWDM on the finite lattice. In particular, we focus on the zero-energy edge modes. By diagonalizing the system Hamiltonian, we obtain the phase diagram including nontrivial topological phases in the $(\alpha - \Delta)$ plane. We have used the existence of the zero-energy edge modes to identify topological phases.

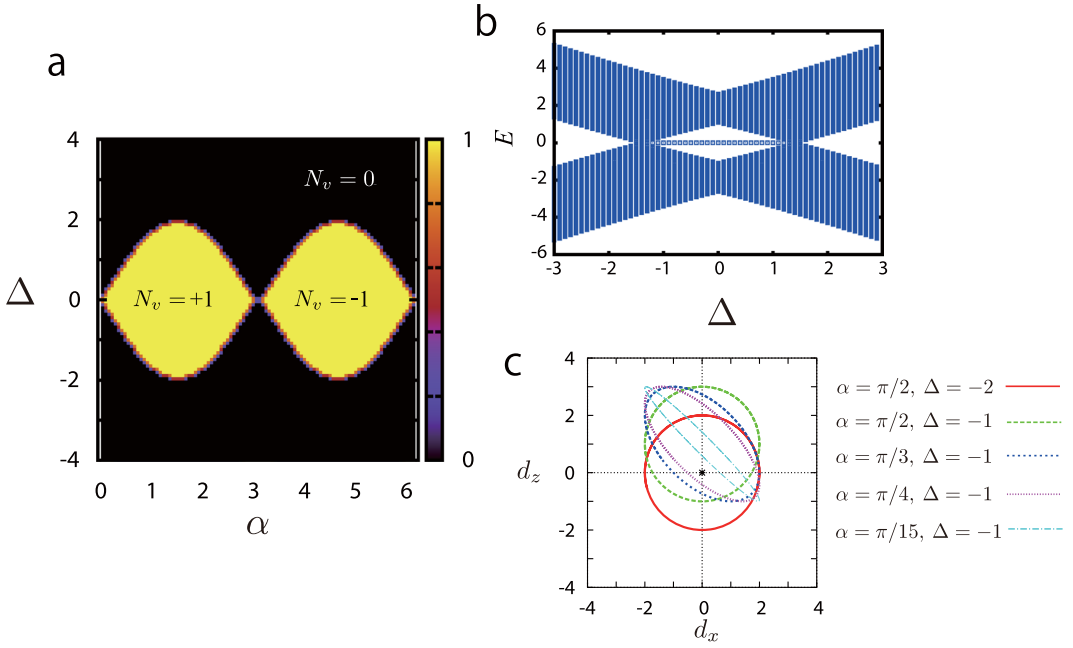

Figure 5. (**a**) Phase diagram of the 1D GWDM for $\theta^a = \theta^b \pm \pi$, $\theta^+ = -\theta^-$, and $\alpha \equiv \theta^- - \theta^a$. The phase diagram has a similar structure to that of the Haldane model on a honeycomb lattice. Δ and α are free parameters. (**b**) Energy spectra with a zero-energy edge state at $\alpha = \pi/4$. (**c**) Hamiltonian trajectories when sweeping k. $\theta^a = \theta^b \pm \pi$, $\theta^+ = -\theta^-$, and $\alpha \equiv \theta^- - \theta^a$. $(d_x, d_z) = (0, 0)$ is the gap closing point in our model.

The obtained phase diagram for $\theta^+ = -\theta^-$ is shown in Fig. 5(a) and a typical energy spectrum in the finite lattice system is shown in Fig. 5(b). In this case, the rotated Pauli matrix reduces to the original one, i.e. $\tilde{\sigma}_x((\theta^+ + \theta^-)/2) \to \sigma_x$. As expected, there exist two topologically nontrivial phases, and they are labeled by the winding number $N_w = \pm 1$. Interestingly, the obtained phase diagram is similar to that of the Haldane model[36,37]. Analytically, the phase boundaries between the trivial ($N_v = 0$) and nontrivial topological phases ($N_w = \pm 1$) are given by $\Delta = \pm \sin\alpha$. Compared to the Haldane model, the present topological phases are characterized by N_w and not the Chern number, whereas α seems to correspond to the "flux parameter" of the Haldane model. At $\alpha = \pi/2$ or $\alpha = 3\pi/2$, if $\theta_a = 0$, the 1D GWDM reduces to the ordinary 1D Wilson-Dirac model. The typical trajectories of $\mathrm{d}(k) = (d_x(k), d_z(k)) \equiv (2\cos k, \Delta - 2\cos(k - \alpha))$ obtained by sweeping k are plotted in Fig. 5(c), which gives the winding number N_w, and in the Boch vector space, $(d_x, d_z) = (0, 0)$ corresponds to the gap closing point. From this plot, we can obtain the winding number N_w [Eq. (14)] from the bulk momentum Hamiltonian.

It is interesting to see the phase diagrams corresponding to the "nontrivial" case with the rotated Pauli matrix $\tilde{\sigma}_x(\theta)$ in [Eqs (19), (24)]. To this end, we fix $\theta_a = 0$, $\theta_b = \pi$ and $\theta^+ = 0$; then, the remaining parameters are θ^- and Δ. The obtained phase diagram is shown in Fig. 6(a). The 1D GWDM on the finite lattice has a topological phase diagram including a broad regime of nontrivial topological phase with $N_w = +1$, and there exist clear edge modes as seen in Fig. 6(b). From the results in Figs 5 and 6, we conclude that if the CS condition Eq. (18) is satisfied, nontrivial topological phases form in rather broad parameter regimes. This fact exhibits flexibility for the actual experimental realization of the 1D GWDM as a quantum simulator of a 1D topological insulator.

Topological charge pumping and the realization of the 1D lattice Gross-Neveu model. A topological pump can be realized in the 1D GWDM by adding a CS breaking term. As an example, the 1D GWDM, which satisfies the CS condition in Eq. (18) and also $\theta^+ = \theta^-$, can be a topological charge-pump model by adding a σ_y-channel term to the GWDM. Explicitly, the σ_y-channel term associated with $\tilde{\sigma}_y(\theta^+)$ is given by

$$H_{\sigma_y} = M \sum_j \Psi_j^\dagger \tilde{\sigma}_y(\theta^+) \Psi_j, \tag{25}$$

where M is the coupling constant of the σ_y channel. In experiments, this term can be created by using another laser-assisted hopping scheme, as shown in Methods. With the term in Eq. (25), the bulk-momentum Hamiltonian of Eq. (21) is changed to

$$H_{\mathrm{bulk}}^{\mathrm{P}}(k) = [\Delta - 2\cos(k + \theta_a)]\sigma_z + [2\sin k]\tilde{\sigma}_x(\theta^+) + M\tilde{\sigma}_y(\theta^+). \tag{26}$$

As we vary the parameters Δ and M adiabatically with the period T, such as

$$(\Delta, M) \to (\Delta\cos(2\pi t/T), M\cos(2\pi t/T))$$

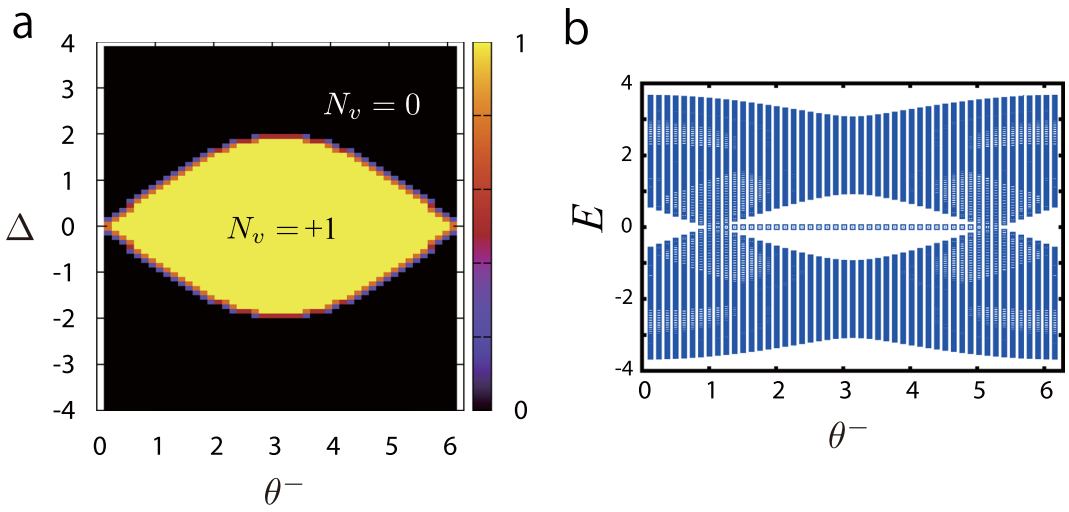

Figure 6. (**a**) Phase diagram of the existence of the zero-energy edge state for $\theta^a = \theta^b \pm \pi = 0$ and $\theta^+ = 0$. θ^- and Δ are free parameters. (**b**) Energy spectra for $\Delta = 1$

[here, $T \gg 1$ for the adiabatic condition], then the model in Eq. (26) is expected to exhibit topological charge pumping phenomena. The phenomena can be observed by measuring the bulk-particle current, which corresponds to a shift in the center of the Wannier function at an optical lattice site[15,16]. A similar argument can be applied to a more general case of the 1DGWDM.

It is interesting to include the interactions between atoms, in particular, those between the different internal states. The interspecies interactions such as,

$$\sum_j V a_j^\dagger a_j b_j^\dagger b_j$$

with a coupling constant V can be expressed in terms of spinor notation Ψ_j as,

$$V_{\text{int}} = \sum_j V a_j^\dagger a_j b_j^\dagger b_j = \sum_j \frac{V}{2} (\Psi_j^\dagger \gamma_0 \Psi_j)^2 . \tag{27}$$

Then, the model $H_{\text{WDM}} + V_{\text{int}}$ is nothing but the lattice version of the Gross-Neveu model[38], which plays an important role in quantum field theory and elementary particle physics. Even in $(1+1)$ D, the Gross-Neveu model has a nontrivial phase diagram with a phase transition. A similar model to the above has been proposed in ref.[24] by using an optical superlattice. In real experiments, ^{173}Yb atom, for example, is a candidate, which has finite s-wave scattering length between the two different internal states in $^1S_0$, whereas the ^{171}Yb atom has a much smaller on-site interaction. Although adding the interaction term disturbs the conditions of lasers in laser-assisted hopping, the fine-tuning of lasers may allow one to realize a quantum simulator of the Gross-Neveu model.

Discussion

In this work, we theoretically proposed the realization of the 1D generalized Wilson-Dirac Hamiltonian in a tilted optical lattice. A combination of two parallel optical lattices with the same tilt and laser-assisted hopping is employed for the atomic quantum simulation of the system. As a concrete example, we suggested ^{171}Yb fermionic atom and also the candidates of energy levels to be used in laser-assisted hopping. The model can be a quantum simulator of a 1D topological insulator.

Next, we studied the GWDM from the view point of symmetry classification theory, which plays an important role in searching for topologically nontrivial phases. Interestingly enough, we found that the CS condition is a sufficient condition that makes the 1D GWDM belong to the BDI class, and we verified this observation by numerically calculating the energy spectra and winding number. This result is important as it shows the flexibility and versatility of the 1D GWDM, i.e. we do not need to create the exact 1D Wilson-Dirac model in experiments as long as we focus on constructing a quantum simulator of a 1D topological insulator.

We obtained the phase diagrams of the model including nontrivial topological phases, and found that some of them have a feature similar to that of the Haldane model.

Finally, we showed that the 1D GWDM possibly exhibits the topological charge pumping if the rotated σ_y-channel is included in this model. We also suggested that by adding inter-species interactions, the model can be a quantum simulator of the lattice version of Gross-Neveu model[38]. Analysis of the 1D GWDM with many-body interactions is an important subject and is expected to lead to richer nontrivial phases. We hope that the proposal in this work will be used for the realization of atomic quantum simulators of 1D Dirac fermion physics for observing, e.g. the Zitterbewegung phenomena in lattice systems[23,39–42], and other related models[22,43].

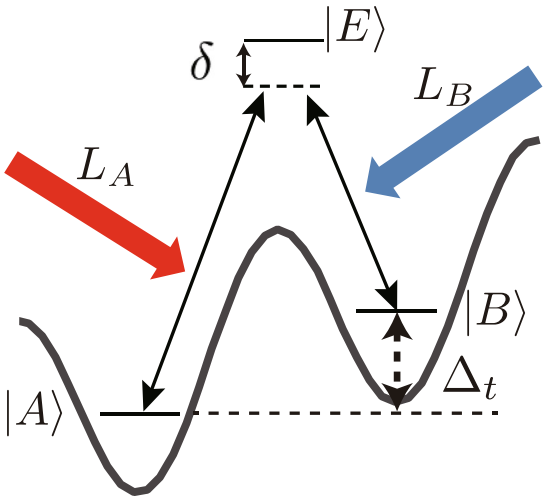

Figure 7. Λ-shaped schema.

Methods

Laser-assisted hopping: General case. To generate the hopping terms in Eqs (8)–(11) in the 1D GWDM, we use excitation lasers in addition to the optical lattice lasers and generate laser-assisted hopping[17,28,34,44–50]. This method is the standard method to create NN hoppings with a nontrivial phase. In general, three states with different energy levels are considered; then, laser-assisted hopping is generated by using Λ-shaped scheme through Rabi coupling[49]. Here, we explain the single Λ-shaped scheme proposed in refs[28,45,51,52].

First, as shown in Fig. 7, we consider two quantum states with different energy levels and different positions denoted by $|A\rangle$ and $|B\rangle$, and one excited state $|E\rangle$. The energy gap between $|A\rangle$ and $|B\rangle$ is denoted by ω_{AB}, and the energy gaps between $|A\rangle$ and $|E\rangle$, and between $|B\rangle$ and $|E\rangle$ are denoted by ω_{AE} and ω_{BE}, respectively. Then by using two excitation lasers L_A and L_B, we can couple $|A\rangle$ and $|B\rangle$ to $|E\rangle$. Here, $L_{A(B)}$ is set at the detuned-frequency $\omega_{AE(BE)} - \delta$, where δ is the detuning with $\delta \ll \omega_{AE(BE)}$ and $\delta \gg \Gamma_E$, where Γ_E is the natural width of $|E\rangle$, and has the wave vector $k_{A(B)}$, which is determined by $|\mathrm{k}_{A(B)}| = (\omega_{AE(BE)} - \delta)/c$ (c is the speed of light). From the two excitation lasers, Rabi coupling can be generated through an electric dipole interaction. The Rabi couplings are denoted by Ω_{AE} and Ω_{BE}. In this setup, we can estimate the effects of the excited state $|E\rangle$ by using the second-order perturbation analysis. Consequently, the coupling between $|A\rangle$ and $|B\rangle$ is effectively generated. In the single particle picture, the coupling constant between $|A\rangle$ and $|B\rangle$ in the rotating frame is given by $\frac{\Omega'_{AE}\Omega'_{BE}}{4\delta}$. A detailed calculation is shown in Supplementary Materials.

Next, the single Λ-shaped scheme is applied to a 1D tilted deep single optical lattice, and we consider laser-assisted hopping. The lattice tilt and deep lattice-depth suppress the natural tunneling between NN lattice sites. The lattice tilt can be engineered, e.g. by using a magnetic field gradient, an electric field (light-shift) gradient and gravity, and leads to an energy difference Δ_t between each pair of NN lattice sites. Then, the application of L_A and L_B to the entire system triggers a Λ-shaped transition of each NN lattice sites. Therefore, if we put non-interacting atoms in the 1D lattice, the tight-binding model is effectively given by

$$H^{2nd(g)} = \sum_j (\tilde{J}_{j,j+1} g^\dagger_{j+1} g_j + \mathrm{h.c.}), \tag{28}$$

$$\tilde{J}_{j,j+1} = \frac{|\Omega'_{AE}||\Omega'_{BE}|}{4\delta} \times \int d\mathrm{r}\, W^*(\mathrm{r} - \mathrm{r}_{j+1}) e^{\delta \mathrm{k}\cdot\mathrm{r}} W(\mathrm{r} - \mathrm{r}_j), \tag{29}$$

where $g^\dagger_j (g_j)$ is a creation (annihilation) operator of an atom on lattice site j, and $\tilde{J}_{j,j+1}$ is a complex hopping parameter determined by a localized wave function $W(\mathrm{r}) \equiv w^{ws}(x)w(y)w(z)$. Here, $w^{ws}(x)$ is the Wannier-Stark state[52,53], determined by the tilted optical lattice and, $w(y)$ and $w(z)$ are the Wannier states, determined by the y- and z-direction optical lattices, which create a strong confinement potential creating a 1D system. δk is defined as $\delta k = k_A - k_B$. By appropriate tuning of the incident angles of the excitation lasers, δk can be uniform along the 1D lattice. Here, it is noted that in Eq. (29), if we set $\omega_{BE} - \omega_{AE} \sim \Delta_t$, the tilt energy difference Δ_t between NN sites does not appear owing to the rotating wave approximation (RWA) with the rotating frame of ω_{AB}[34]. The hopping terms in Eq. (28) are a basic ingredient for the creation of the hopping terms in Eqs (8)–(11).

Uniform phase creation. The phase created when in applying laser-assisted hopping is spatially dependent since the phase is determined by δk as in Eq. (29). However, since our target model is 1D, if we prepare a three dimensional cubic optical lattice, 1D optical lattice chains with uniform phases are created by making the remaining lattice potential sufficiently deep to confine atoms with many 1D tubes. When the direction of 1D tube in this lattice configuration is regarded as the x-direction, the condition $\delta \mathrm{k} = (0, k^y_A - k^y_B, k^z_A - k^z_B)$ leads to a uniform

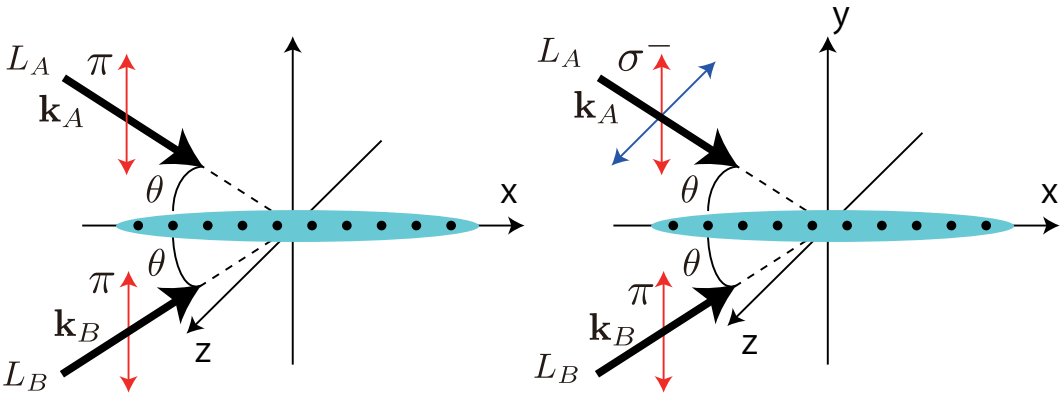

Figure 8. Schematics of the incident lasers for laser-assisted hopping. The quantization axis is in the *x*-direction.

phase along the *x*-direction, even though the value of the uniform phase of each tube is different. Figure 8 shows schematics of incident lasers for the laser-assisted hopping with the uniform phase. The blue ellipses represent a 1D gas trapped in two parallel optical lattice. The left panel shows two types of laser-assisted hopping, $\Lambda^{a_j}_{a_{j+1}}$ and $\Lambda^{b_j}_{b_{j+1}}$. Similarly, the right panel shows two types of laser-assisted hopping, $\Lambda^{a_j}_{b_{j+1}}$ and $\Lambda^{a_j}_{b_{j-1}}$. Both cases create the hopping with the uniform phase along the *x*-direction.

Rotational transformed Pauli matrix. The Pauli matrix can be transformed by performing a rotational transformation in the spin space. The full rotation of the spin space is determined by two rotational angles. In general, the rotated Pauli matrix $\tilde{\sigma}_j$ along the *i*-component spin ($i=1(x), 2(y), 3(z)$) axis is given by a formula incorporating the rotational angle ρ:

$$\tilde{\sigma}_j(\rho) \equiv e^{-i\rho\sigma_i/2}\sigma_j e^{i\rho\sigma_i/2} = \sigma_j \cos\rho + \varepsilon_{ijk}\sigma_k \sin\rho. \tag{30}$$

If one takes $(i, j, k) = (3, 1, 2)$, and sets $\rho = \phi$, the rotated *x*- and *y*-component Pauli matrices rotated around the *z*-spin axis are given as

$$\tilde{\sigma}_x(\phi) \equiv \begin{bmatrix} 0 & e^{i\varphi} \\ e^{-i\phi} & 0 \end{bmatrix}, \tag{31}$$

$$\tilde{\sigma}_y(\phi) \equiv \begin{bmatrix} 0 & -ie^{i\phi} \\ ie^{-i\phi} & 0 \end{bmatrix}. \tag{32}$$

The rotated sigma matrices $(\tilde{\sigma}_x(\phi), \tilde{\sigma}_y(\phi), \sigma_z)$ also satisfy the SU(2) commutation relation. By the complex conjugate transformation $\mathcal{K}$,

$$\mathcal{K}\tilde{\sigma}_x(\phi)\mathcal{K} = \tilde{\sigma}_x(-\phi). \tag{33}$$

References

1. Georgescu, I. M., Ashhab, S. & Nori, F. Quantum simulation. *Rev. Mod. Phys.* **86**, 153 (2014).
2. Ryder, L. H. *Quantum Field Theory* (Cambridge University Press, Cambridge, 1985).
3. Rothe, H. J. *Lattice Gauge Theories: An Introduction* (World Scientific, 2005).
4. Wen, X.-G. Quantum Field Theory of Many-body Systems: From the Origin of Sound to an Origin of Light and Electrons, Oxford Graduate Texts (OUP Premium, New York, 2004).
5. Shen, S.-Q. *Topological Insulators* (Springer-Verlag, Berlin, 2012).
6. Asboth, J. K., Oroszlany, L., & Palyi, A. *A Short Course on Topological Insulators: Band Structure and Edge States in One and Two Dimensions* (Springer, Berlin, 2016).
7. Zhu, S. L., Wang, Z. D., Chan, Y. H. & Duan, L. M. Topological Bose-Mott Insulators in a One-Dimensional Optical Superlattice. *Phys. Rev. Lett.* **110**, 075303 (2013).
8. Deng, X. & Santos, L. Topological transitions of interacting bosons in one-dimensional bichromatic optical lattices. *Phys. Rev. A.* **89**, 033632 (2014).
9. Lang, L. J., Cai, X. & Chen, S. Edge States and Topological Phases in One-Dimensional Optical Superlattices. *Phys. Rev. Lett.* **108**, 220401 (2012).
10. Matsuda, F., Tezuka, M. & Kawakami, N. Topological Properties of Ultracold Bosons in One-Dimensional Quasiperiodic Optical Lattice. *J. Phys. Soc. Japan* **83**, 083707 (2014).
11. Xu, Z., Li, L. & Chen, S. Fractional Topological States of Dipolar Fermions in One-Dimensional Optical Superlattices. *Phys. Rev. Lett.* **110**, 215301 (2013).
12. Ganeshan, S., Sun, K. & Das Sarma, S. opological Zero-Energy Modes in Gapless Commensurate Aubry-Andre-Harper Models. *Phys. Rev. Lett.* **110**, 180403 (2013).

13. Hu, H., Cheng, C., Xu, Z., Luo, H. G. & Chen, S. Topological nature of magnetization plateaus in periodically modulated quantum spin chains. *Phys. Rev. B* **90**, 035150 (2014).
14. Song, B. *et al*. Observation of symmetry-protected topological band with ultracold fermions. *Science Advances* **4**, eaao4748 (2018).
15. Nakajima, S. *et al*. Topological Thouless Pumping of Ultracold Fermions. *Nat. Phys.* **12**, 296 (2016).
16. Lohse, M., Schweizer, C., Zilberberg, O., Aidelsburger, M. & Bloch, I. A Thouless Quantum Pump with Ultracold Bosonic Atoms in an Optical Superlattice. *Nat. Phys.* **12**, 350 (2016).
17. Mancini, M. *et al*. Observation of chiral edge states with neutral fermions in synthetic Hall ribbons. *Science* **349**, 981 (2015).
18. Wilson, K. G. In: *New Phenomena* in *Subnuclear Physics* (Erice, 1975), ed. Zichichi A. (Plenum, New York, 1977).
19. Galitski, V. & Spielman, I. B. Spin-orbit coupling in quantum gases. *Nature (London)* **494**, 49–54 (2013).
20. Ruostekoski, J., Dunne, G. V. & Javanainen, J. Particle Number Fractionalization of an Atomic Fermi-Dirac Gas in an Optical Lattice. *Phys. Rev. Lett.* **88**, 1804011 (2002).
21. Zheng, Z., Pu, H., Zou, X. & Guo, G. Artificial topological models based on a one-dimensional spin-dependent optical lattice. *Phys. Rev. A* **95**, 013616 (2017).
22. Bermudez, A. *et al*. Wilson Fermions and Axion Electrodynamics in Optical Lattices. *Phys. Rev. Lett.* **105**, 190404 (2010).
23. Garreau, J. C. & Zehnle, V. Simulating Dirac models with ultracold atoms in optical lattices. *Phys. Rev. A* **96**, 043627 (2017).
24. Cirac, J. I., Maraner, P. & Pachos, J. K. Cold Atom Simulation of Interacting Relativistic Quantum Field Theories. *Phys. Rev. Lett.* **105**, 190403 (2010).
25. As a similar optical lattice setup, for ^{87}Rb, Soltan-Panahi, P., Struck, J., Hauke, P., Bick, A., Plenkers, W., Meineke, G., Becker, C., Windpassinger, P., Lewenstein, M., & Sengstock, K. Multi-component quantum gases in spin-dependent hexagonal lattices. *Nat. Phys.* **7**, 434 (2011)
26. For ^{173}Yb, Riegger, L., Oppong, N. D., Hofer, M., Fernandes, D., R., Bloch, I., & Folling, S. Localized Magnetic Moments with Tunable Spin Exchange in a Gas of Ultracold Fermions. *Phys. Rev. Lett*. **120**, 143601 (2018).
27. Mandel, O. *et al*. Coherent Transport of Neutral Atoms in Spin-Dependent Optical Lattice Potentials. *Phys. Rev. Lett.* **91**, 010407 (2003).
28. Jaksch, D. & Zoller, P. Creation of effective magnetic fields in optical lattices: the Hofstadter butterfly for cold neutral atoms. *New J. Phys.* **5**, 56 (2003).
29. Grimm, R., Weidenmuller, M. & Ovchinnikov, Y. B. Optical dipole traps for neutral atoms. *Adv. At. Mol. Opt. Phys.* **42**, 95 (2000).
30. Barker, D. S., Pisenti, N. C., Reschovsky, B. J. & Campbell, G. K. Three-photon process for producing a degenerate gas of metastable alkaline-earth-metal atoms. *Phys. Rev. A* **93**, 053417 (2016).
31. Ovsyannikov, V. D., Pal'chikov, V. G., Katori, H. & Takamoto, M. Polarisation and dispersion properties of light shifts in ultrastable optical frequency standards. *Quantum Electron.* **36**, 3 (2006).
32. Ryu, S., Schnyder, A. P., Furusaki, A. & Ludwig, A. W. W. Topological insulators and superconductors: ten-fold way and dimensional hierarchy. *New J. Phys.* **12**, 065010 (2010).
33. Kitaev, A. Periodic table for topological insulators and superconductors. *AIP Conf. Proc.* **1134**, 22 (2009).
34. Miyake, H. Probing and Preparing Novel States of Quantum Degenerate Rubidium Atoms in Optical Lattices. *Ph.D. thesis, Massachusetts Instittute of Technology* (2013).
35. Ryu, S. & Hatsugai, Y. Topological Origin of Zero-Energy Edge States in Particle-Hole Symmetric Systems. *Phys. Rev. Lett.* **89**, 77002 (2002).
36. Similar result in Li, L., Xu, Z. & Chen, S. Topological phases of generalized Su-Schrieffer-Heeger models. *Phys. Rev. B* **89**, 085111 (2014).
37. Haldane, F. D. M. Model for a Quantum Hall Effect without Landau Levels: Condensed-Matter Realization of the "Parity Anomaly". *Phys. Rev. Lett.* **61**, 2015 (1988).
38. Gross, D. J. & Neveu, A. Dynamical symmetry breaking in asymptotically free field theories. *Phys. Rev. D* **10**, 3235 (1974).
39. Vaishnav, J. Y. & Clark, C. W. Observing Zitterbewegung with Ultracold Atoms. *Phys. Rev. Lett.* **100**, 153002 (2008).
40. Merkl, M., Zimmer, F. E., Juzeliunas, G. & Ohberg, P. Atomic Zitterbewegung. *EPL* **83**, 54002 (2008).
41. Qu, C., Hamner, C., Gong, M., Zhang, C. & Engels, P. Observation of Zitterbewegung in a spin-orbit-coupled Bose-Einstein condensate. *Phys. Rev. A* **88**, 021604(R) (2013).
42. Leblanc, L. J. *et al*. Direct observation of zitterbewegung in a Bose-Einstein condensate. *New J. Phys.* **15**, 073011 (2013).
43. Gholizadeh, S., Yahyavi, M. & Hetényi, B. Extended Creutz ladder with spin-orbit coupling: a one-dimensional analog of the Kane-Mele model. *EPL* **122**, 27001 (2018).
44. Aidelsburger, M. *et al*. Realization of the Hofstadter Hamiltonian with Ultracold Atoms in Optical Lattices. *Phys. Rev. Lett.* **111**, 185301 (2013).
45. Miyake, H., Siviloglou, G. A., Kennedy, C. J., Burton, W. C. & Ketterle, W. Realizing the Harper Hamiltonian with Laser-Assisted Tunneling in Optical Lattices. *Phys. Rev. Lett.* **111**, 185302 (2013).
46. Gerbier, F. & Dalibard, J. Gauge fields for ultracold atoms in optical superlattices. *New J. Phys.* **12**, 033007 (2010).
47. Dalibard, J., Gerbier, F., Juzeliunas, G. & Ohberg, P. Colloquium: Artificial gauge potentials for neutral atoms. *Rev. Mod. Phys.* **83**, 1523 (2011).
48. Lin, Y. J. *et al*. Bose-Einstein Condensate in a Uniform Light-Induced Vector Potential. *Phys. Rev. Lett.* **102**, 130401 (2009).
49. Goldman, N., Juzeliunas, G., Ohberg, P. & Spielman, I. B. Light-induced gauge fields for ultracold atoms. *Rep. Prog. Phys.* **77**, 126401 (2014).
50. Celi, A. *et al*. Synthetic Gauge Fields in Synthetic Dimensions. *Phys. Rev. Lett.* **112**, 043001 (2014).
51. Keilmann, T., Lanzmich, S., McCulloch, I. & Roncaglia, M. Statistically induced phase transitions and anyons in 1D optical lattices. *Nat. Commun.* **2**, 361 (2011).
52. Greschner, S. & Santos, L. Anyon Hubbard Model in One-Dimensional Optical Lattices. *Phys. Rev. Lett.* **115**, 053002 (2015).
53. Gluck, M., Kolovsky, A. R., Korsch, H. J. & Moiseyev, N. Calculation of Wannier-Bloch and Wannier-Stark states. *Eur. Phys. J. D* **4**, 239 (1998).

Acknowledgements

We thank T. Fukui for providing us inspiration for this study. Y. K. acknowledges the support of a Grant-in-Aid for JSPS Fellows (No. 17J00486). This work was partially supported by a Grant-in-Aid for Scientific Research from the Japan Society for the Promotion of Science under Grant Nos. 25220711, 16H00990, 16H00801, and 17H06138, the Impulsing Paradigm Change through Disruptive Technologies (ImPACT) program, and JST CREST (No. JPMJCR1673).

Author Contributions

Y.K. considered the basic ideas of the work and carried out all the theoretical analysis and calculations. I.I. and Y.T. discussed the theoretical and experimental parts, respectively. All authors contributed to the writing of the manuscript.

Additional Information

Supplementary information accompanies this paper at https://doi.org/10.1038/s41598-018-29143-w.

Competing Interests: The authors declare no competing interests.

Publisher's note: Springer Nature remains neutral with regard to jurisdictional claims in published maps and institutional affiliations.